A Study on Flow Transition and Development in Circular and Rectangular Ducts

E.-S. Zanoun
Department of Aerodynamics and Fluid Mechanics,
Brandenburg University of Technology Cottbus,
Siemens-Halske-Ring 14,
D-03046 Cottbus, Germany

M. Kito
Mie University,
1577 Kurimamachiya-cho,
Tsu City,
Mie Prefecture, Japan

C. Egbers
Department of Aerodynamics and Fluid Mechanics,
Brandenburg University of Technology Cottbus,
Siemens-Halske-Ring 14,
D-03046 Cottbus, Germany

The present paper reports observations on some aspects regarding the dependence of the transition Reynolds number and flow development on the inlet flow conditions and the entrance length in circular and rectangular ducts for $Re_m \leq 106 \times 10^3$, where Re_m is the Reynolds number based on the bulk flow velocity ($\bar{U}_b$) and the duct integral length scale (D). The hot-wire anemometer was used to carry out measurements close to the circular duct exit; however, the laser-Doppler anemometry was utilized for the rectangular duct measurements. Particular considerations were given to the bulk flow velocity, the mean-velocity profile, the centerline-average-velocity, and the centerline turbulence statistics to the fourth order. Transition criteria in both ducts were discussed, reflecting effects of flow geometry, entrance flow conditions, and entrance length on the transition Reynolds number. A laminar behavior was maintained up to $Re_m \approx 15.4 \times 10^3$ and $Re_m \approx 2 \times 10^3$ in the circular and rectangular ducts, respectively, and the transition was observed to take place at different downstream positions as the inlet flow velocity varied.
[DOI: 10.1115/1.3112384]

Keywords: circular and rectangular ducts, flow transition and development

1 Introduction and Aim of the Work

Transitional flows either in circular or rectangular ducts are encountered in a variety of industrial applications, and therefore a correct prediction of flow transition is of vital importance, for instance, in flow control either trying to delay or to have an early transition to turbulence. Flow transition in the circular ducts, i.e., pipes, goes back to 1883 when Osborne Reynolds performed his well-known circular pipe flow experiment. He observed that the pipe flow, depending on a dimensionless number later named the Reynolds number, consists of basically two different states, either laminar or turbulent. Reynolds also found that the transition from the laminar to turbulent state sets in intermittently by “flashes” that occur in localized regions when the Reynolds number exceeds a so-called “critical” value. As the Reynolds number increases, the frequency of these “flashes” increases until a state of fully developed turbulence is obtained in the downstream direction of the so-called core region. All these fundamental properties of the pipe flow were later found to represent some common features of wall-bounded shear flows where velocity and temperature gradients and geometry of flows change. However, the detailed process and mechanism involved in the transition of the circular pipe flow are still under progress. Significant international collaboration has been therefore recognized, trying to understand its physics of transition [1–6]. Some more detailed experimental and theoretical progress about the pipe flow transition have been reviewed by Kerswell [7] and given, recently, by Willis et al. [8]. Different scenarios, for instance, the transient growth of disturbances proposed by Trefethen et al. [9] or the so-called self-sustained process (SSP) introduced by Waleffe [10], and recently the nonlinear traveling wave [3,4], may be considered appropriate processes to explain the pipe flow transition. Besides, earlier extensive experiments have been conducted by Wygnanski and Champagne [11] and Wygnanski et al. [12], identifying two types of structures in the transitional pipe flow, which they called puffs and slugs. Figure 1 illustrates some selected samples of the streamwise traces from the hot wire, located at the pipe centerline (see Fig. 2(*a*)), for various inlet flow velocities, showing the laminar, intermittent, and fully turbulent flows. At $x/D=70.2$, for $Re_m \approx 3{,}700$ and 12,300, a laminar behavior was observed and at $x/D=27.3$ as the inlet flow velocity increases the flow transition to turbulent regime occurred passing through an intermittent flow with 0.44% intermittency for $Re_m \approx 27{,}800$. It is worth noting that the transition from the laminar to turbulent regime in the present pipe flow has been carried out naturally, i.e., without triggering the flow at the pipe entrance.

Transition of such kind of flows was found to depend, for instance, on the smoothness of the inlet contraction, triggering the flow at the entrance, the surface roughness of the test section, and therefore on the minimum entrance length (L) required for flow to develop. Hence, the flow usually reaches the fully developed state when all mean flow quantities (i.e., velocity and pressure fields) and all turbulence quantities (i.e., $\overline{u'^2}$, skewness, flatness, spectra, etc.) become invariant with the streamwise location, see Zagarola and Smits [13]. However, a discrepancy through investigations [14–19] concerning criterion on the minimum entrance length needed to assure the state of the fully developed turbulent flow still exists. For example, Nikuradse [14] concluded by comparing the mean-velocity profiles at successive streamwise distances from the pipe inlet that flow was fully developed turbulent between $25D$ and $40D$, where D stands either for the pipe diameter or the channel full height. In a similar way, Laufer [20] claimed a pipe full development length of $30D$ based on the measured mean-velocity distributions. For axisymmetry disturbances, pipe flow experiments by Sarpkaya [15] yield $x/D=30$ before reaching the fully developed region, and the analysis by Haung and Chen [16,17] predicts $x/D=32$ for the fully developed state. However, for the nonaxisymmetric disturbances, a development length was found by Haung and Chen [16,17] to lie between $40D$ and $48D$ and through flow triggering at the pipe entrance using the wall fence type; their critical Reynolds number was 2300. Perry and Abel [18] observed a fully developed state at $71.9D$ and $86.2D$ with triggering the flow at the pipe entrance for $Re_m=3\times10^5$. Patel and Head [21] concluded that both the mean and the fluctu-

Contributed by the Fluids Engineering Division of ASME for publication in the Journal of Fluids Engineering. Manuscript received February 27, 2008; final manuscript received February 17, 2009; published online xxxxx-xxxxx-xxxxx. Assoc. Editor: Juergen Kompenhans.

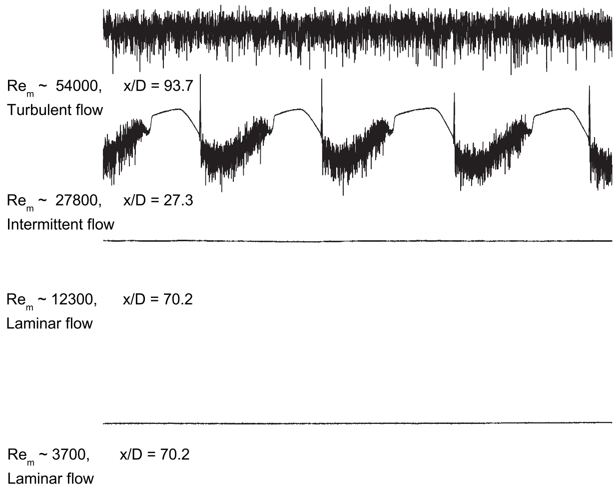

Fig. 1 Some selected samples of the streamwise traces from the hot-wire anemometer, located at the pipe centerline, for various inlet flow velocities and streamwise locations

ating velocity distributions in a turbulent pipe flow indicate a full development state for a downstream distance of 50–80D. Lien et al. [19] indicated that a minimum channel length of 130D is required for flow to become sensibly constant with the streamwise direction. More recently, Doherty et al. [22] noted that the mean-velocity profiles required development length over $x/D \approx 50$ to become invariant; however, a streamwise distance of $x/D \approx 80$ for higher order statistics is needed. Figure 2(b) shows a summary of the normalized total pipe length (L/D) from some existing and planned experimental pipe test facilities.

In spite of the above significant efforts, no quite clear entrance length criterion was assumed for the fully developed flow either in the pipe or in the channel flows. However, it becomes common in the fluid mechanics community to exceed the entrance length by large enough x/D to assure the state of full development of the flow. Therefore, aiming at better understanding and developing criteria for flow transition and development in both the pipe and the channel facilities, a comparative study between the two types of flows was carried out. The present experimental studies are therefore carried out with particular attention being given to the centerline measurements for low range of Reynolds numbers, $\mathrm{Re}_m \leq 106 \times 10^3$, and to assure that the selection of the measuring section $L/D=85$ of Zanoun et al. [23] was appropriate and enough far away from the contraction exit to assume fully developed turbulent pipe flow.

The outline of the present paper can be briefly described as follows. Section 2 describes the pipe experimental test facility and the measuring techniques. The data presented in Sec. 3 resulted from both the present pipe experimental measurements and some available channel flow data [24]. Finally, conclusions and final remarks are drawn and suggestions for further work have been reported in Sec. 4.

2 Experimental Apparatus and Measuring Techniques

The Department of Aerodynamics and Fluid Mechanics (LAS) at BTU Cottbus maintains a high quality aeroacoustic test facility for the sake of research and development, see Fig. 3. The aeroacoustic test facility is laid out openly, i.e., free jet without direct feedback, and it is mainly designed for aeroacoustic applications; see Ref. [25] for more details. The facility uses a radial fan to provide air with a maximum velocity of 60 m/s at the nozzle exit with centerline turbulence intensity level less than 0.35%; see Fig. 4. For the sake of carrying out the present work, a pipe test section was added to the test facility in the measuring room~~,~~ as Fig. 3 indicates. The pipe test section was made out of a high-precision smooth acrylic-glass tube that was connected directly to a carefully machined two-cubic arcs exit nozzle, having an aspect ratio of 8. The nozzle was used between the plenum chamber and the pipe test section to assure a smooth and uniform inlet flow in addition to damping further any flow disturbances coming from the plenum chamber. The geometric dimensions of the pipe showed an internal diameter, D, of 32 mm and total length, L, of 6 m, providing total pipe length-to-diameter ratio of $L/D=187.5$. The pipe consisted of various sections connected together by custom-designed couplings. Measurements of the mean-velocity profiles, the bulk flow velocity, the centerline-average-velocity, and the centerline-velocity fluctuations were made at several stations along the pipe section between $x/D=3.9$ and 156. It is worth mentioning that all measurements were carried out without triggering the flow at the pipe inlet, and here is a summary of the different measuring locations

$$x/D = 3.90, 7.81, 11.72, 15.60, 19.53, 23.44, 27.34, 31.25, 35.16,$$
$$38.97, 46.78, 54.59, 62.40, 70.20, 78.00, 93.66, 108, 125, 140,$$
$$156$$

The pipe flow rate for each investigated case was controlled by changing the rotational speed of a 5.5 kW radial fan via a fre-

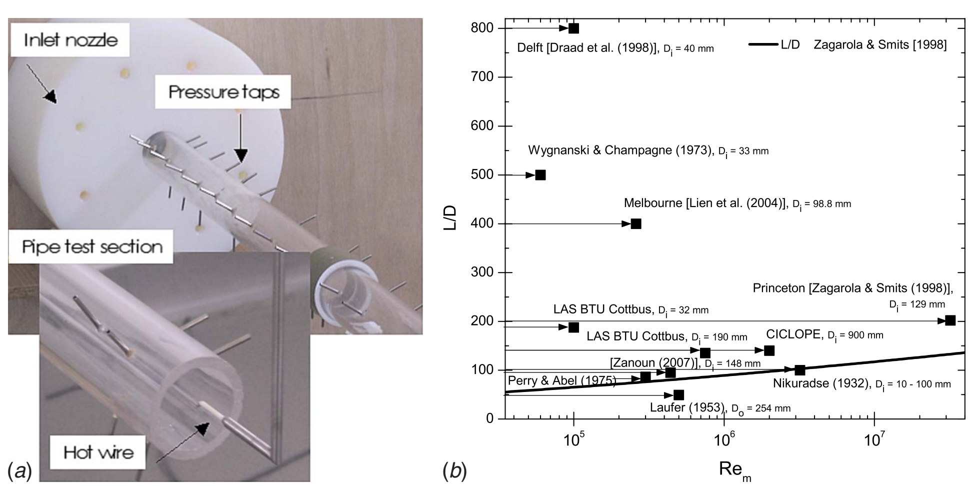

Fig. 2 (a) Photograph of the current pipe test section and (b) summary of the L/D versus the mean-based Reynolds number, Re$_m$, from some existing and planned pipe facilities

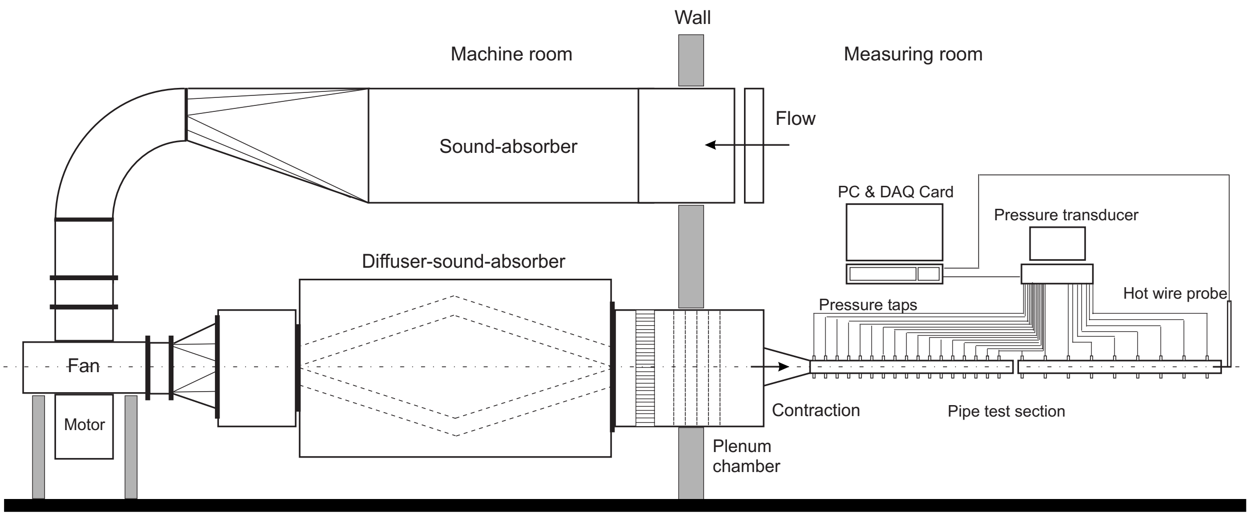

Fig. 3 Schematic of the experimental test facility

quency converter unit. A conventional one-dimensional laser-Doppler anemometry (LDA), FlowLite System Dantec Dynamics GmbH, operating in the dual-beam backscattering mode was used to calibrate the wind tunnel. The bulk flow velocity, $\bar{U}_b$, was measured using the LDA at the contraction exit, where a uniform velocity distribution exists. In addition, it was also obtained by integrating the velocity profile at the measuring location for each Reynolds number to ensure a good assessment of the bulk flow velocity for each case. Good agreement of about $\pm 1\%$ was achieved for the average velocity from both methods and the bulk flow velocity was then used to compute the bulk-velocity based Reynolds number of the flow, $\mathrm{Re}_m = \bar{U}_b D/\nu$. A low range of Reynolds numbers, i.e., $\mathrm{Re}_m \leq 106\times 10^3$, was set up in this way. Finally, by careful installation of the pipe test section with the plenum chamber and the contraction using the laser alignment, we were able to limit any misalignment in the test facility.

Intensive measurements utilizing the hot-wire anemometer (HWA) at the above mentioned measuring locations have been carried out with particular attention being given to

- the bulk flow velocity ($\bar{U}_b$) and the centerline-average-velocity ($\bar{U}_c$)
- the centerline turbulence statistics up to the fourth moment (i.e., $\overline{u_c'^2}$, skewness, and flatness)
- the mean-velocity distributions, $\bar{U} = f(y)$
- the mean wall pressure gradient ($\mathrm{d}P/\mathrm{d}x$) and therefore the wall skin friction velocity (u_τ)

The detailed velocity measurements were carried out using a Multi-channel constant-temperature anemometer (CTA) System from Dantec Dynamics GmbH. The hot-wire measurements of the local velocity were made utilizing a boundary layer probe equipped with a 5 μm diameter wire (d) and 1.25 mm an active wire length (ℓ), providing an aspect ratio (ℓ/d) of 250. Hence the wire had a sufficiently large aspect ratio to suggest a negligible influence of the prongs on the actual velocity measurement. All calibrations and measurements were performed with an 80% overheat ratio, $a = (R_w - R_a)/R_a$, where R_w is the operational hot-wire resistance and R_a is the resistance of the cold wire, i.e., at ambient air temperature. For the statistical data analysis of the local flow, $5\times 10^4 \cancel{\times} 10^5$ samples were acquired over 60 s at every measuring point.

The local mean static pressure measurements were employed to evaluate the streamwise pressure gradient ($\mathrm{d}P/\mathrm{d}x$), which in turn was used to obtain the wall shear stress (τ_w) and then the wall friction velocity (u_τ) that needed to normalize the mean-velocity data

$$\tau_w = -\frac{R}{2}\frac{\mathrm{d}P}{\mathrm{d}x} \Rightarrow u_\tau = \sqrt{\frac{\tau_w}{\rho}} \qquad (1)$$

where R is the pipe radius. At each x-location for the streamwise pressure measurements, three static pressure holes of 500 μm were carefully installed around the circumference of the pipe. Care was taken to ensure that the inner surface of the pipe, where the pressure holes were drilled, was free from remaining drilling defects of the holes (i.e., smoothness was ensured around the pressure tappings). The mean static pressure at each location was then obtained by averaging measurements over the three pressure holes. As a result, the wall skin friction data were computed, independently of the mean-velocity profile measurements. A temperature sensor was used to measure the temperature with high accuracy directly at the pipe exit. The ambient pressure was monitored in the laboratory and reported for each test run using Baratron 626A electronic barometric sensor, MKS Instrument GmbH. Utilizing both the mean pressure measurements and the corresponding air stream temperature in the pipe, the air density (ρ) and the kinematic viscosity (ν) were calculated using the ideal gas relationships and Sutherland's correlation [23].

3 Experimental Results and Discussion

There is no doubt that there are remarkable effects for the pipe or the channel inlet flow conditions, geometrical dimensions, and entrance length on flow development, transition location, and transition Reynolds number. To simplify the problem, we summarized here the most relevant parameters that influence the transition from the laminar to turbulent flow regime either in the pipe or in the channel as follows:

$$(x)_{\mathrm{crit}} = f(\bar{U}_c, u_c', D, \epsilon, \rho, \mu) \qquad (2)$$

where f expresses a functional relationship, $(x)_{\mathrm{crit}}$ is the critical entrance length at which transition occurs, $\bar{U}_c$ is the average flow velocity at the pipe or at the channel centerline, u_c' is the centerline turbulence level, D stands either for the pipe or the channel integral length scale, ϵ is the pipe or the channel surface roughness, ρ is the fluid density, and μ is the fluid dynamic viscosity. Equation (2) can be rewritten as follows by carrying out the dimensional analysis:

$$\left(\frac{x}{D}\right)_{\text{crit}} = f\left(\text{Re}_c, \frac{u_c'}{\bar{U}_c}, \frac{\epsilon}{D}\right) \tag{3}$$

stating that the critical entrance length, i.e., transition location, needed for flow transition depends on the entrance Reynolds number (Re_c), the entrance turbulence intensity level ($u_c'/\bar{U}_c$), and the relative surface roughness (ϵ/D). On the other hand, Eq. (3) can be rewritten as follows:

$$(\text{Re}_c)_{\text{crit}} = f\left(\frac{x}{D}, \frac{u_c'}{\bar{U}_c}, \frac{\epsilon}{D}\right) \tag{4}$$

indicating that the transition Reynolds number depends on the dimensionless streamwise distance or the measuring location (x/D), the entrance turbulence intensity level ($u_c'/\bar{U}_c$), and the relative surface roughness (ϵ/D). Even, the critical turbulence intensity level $(u_c'/\bar{U}_c)_{\text{crit}}$ can be represented as a function of Re_c, x/D, and ϵ/D; see, e.g., Figs. 5, 6, 11, and 12. However, the centerline turbulence measurements at different locations have been taken, in the present study, as a transition indicator for the state of flow full development and to specify a value for the transition Reynolds number.

In nature, the pipe or the channel surface roughness does play a role in the flow transition except if the surface is hydraulically smooth. In the present study, we can neither verify nor quantify this influence because we did not change the surface roughness. Therefore, the effect of the roughness was omitted since both the present pipe and the channel of Fischer [24] were hydraulically smooth. In addition, the geometrical dimensions and the contour of the inlet contractions were not subjected to changes during either the current phase of the pipe or the channel experiments [24]. Hence the following relation holds:

$$(\text{Re}_c)_{\text{crit}} = f\left(\frac{x}{D}, \frac{u_c'}{\bar{U}_c}\right) \tag{5}$$

Figure 4 illustrates the pipe inlet turbulence intensity level ($u'/\bar{U} \equiv u_c'/\bar{U}_c$) versus the bulk-velocity based Reynolds number (Re_m), which is equivalent to the centerline-velocity based Reynolds number (Re_c) at the contraction exit, where the velocity profile is uniform. It is natural to assume that finite and even small amplitude perturbations at the pipe or at the channel inlet sections are needed for triggering turbulence; however, these perturbations might become of less importance as the Reynolds number increases; see Fig. 4. At higher input velocities, i.e., high Reynolds numbers, the flow is less stable and therefore any small disturbances at the entrance grow fast due to the higher rate of energy production, leading to flow transition. The perturbations at the contraction exit were observed to inversely proportional to the Reynolds number, i.e., $u_c'/\bar{U}_c \propto \text{Re}_m^{-1}$, as the figure clearly illustrates. This turned out to be in good agreement with the scaling law proposed by Hof et al. [26], indicating that the amplitude of perturbation required to cause transition scales as $O(\text{Re}^{-1})$. Grossman [27] indicated also that the onset of turbulence has a double threshold: ~~both~~ the initial disturbance, measured either by its energy or its amplitude, and the Reynolds number have to be large enough, i.e., the disturbance needed is the smaller the larger the Reynolds number already is and vice versa in agreement with Fig. 4.

From previous investigations we might conclude that the type, the magnitude, and the frequency of the perturbations at the pipe entrance play important roles to characterize the laminar-to-turbulent flow transition. However, in various experiments in which the perturbations of the laminar flow could be, carefully, avoided or considerably reduced, the onset of turbulence can be delayed to high Reynolds numbers. For instance, Reynolds in 1883 concluded from his pipe flow experiment that the transition from the laminar to turbulent flow forms takes place at about the

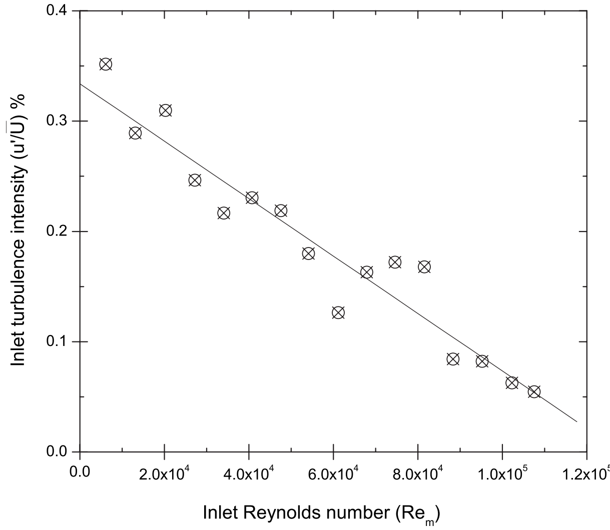

Fig. 4 The turbulence intensity level ($u'/\bar{U}$) versus the bulk-velocity based Reynolds number (Re_m) at the contraction exit~~,~~ without triggering the flow

same Reynolds number, i.e., $(\text{Re}_m)_{\text{crit}}=2300$. However, he observed that at low level of perturbations, the transition Reynolds number could be much larger than the most accepted critical value, i.e., $(\text{Re}_m)_{\text{crit}}=2300$. Investigations by Schiller [28], for instance, have shown laminar behavior at $\text{Re}_m=2\times10^4$. In addition, a recent work by Draad et al. [1] indicated a natural transition at locations between $x/D=788{,}75$ and $807{,}75$ for $\text{Re}_m=6\times10^4$, and their setup was able to sustain a fully developed parabolic pipe flow for Reynolds number up to 14,300. A laminar pipe flow was also observed even at more higher Reynolds number, i.e., $\text{Re}_m=10^5$ [29]. Hence, we might conclude that specifying a numerical value for the transition Reynolds number depends on the boundary conditions of each individual test facility.

Therefore, in addition to the input flow velocity, some other important factors that influence flow transition to turbulence either in the pipe or in the channel flows can be resummarized as follows:

- the level, type, and frequency of disturbances of the inlet flow
- the smoothness, geometry of the entrance, and the wall roughness
- the entrance length, and the alignment of the test section
- the pressure distribution of the internal flow

Now, an important question arises: Is it difficult to have a precise estimation for the transition Reynolds number and consequently a definition for the term fully developed flow? In the past, three different criteria have been used [21] to characterize the fully developed turbulence in pipes or channels:

1. Having a well established relationship between the wall skin friction and the Reynolds number, for instance, obeying the 1/4 power friction relation $\lambda=0.3164\ \text{Re}_m^{0.25}$ of Blasius [30].
2. For Reynolds number much higher than the transition Reynolds number, the measured mean-velocity profiles scaled with the inner wall variables (i.e., the viscous length scale ($\ell_c=\nu/u_\tau$) and the wall friction velocity ($u_c=u_\tau=\sqrt{\tau_w/\rho}$)) collapse and agree well with the well-known logarithmic law of the wall, i.e., $\bar{U}/u_\tau=1/\kappa\ln(yu_\tau/\nu)+B$, showing Reynolds number independence of the mean-velocity data, where κ and B are believed to be universal constants [31].
3. A continuously turbulent flow exists or, in other words, the intermittency factor is equal to 1 [24]. The authors of the

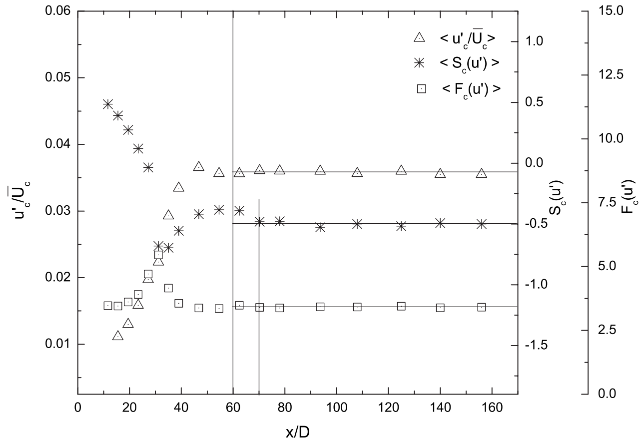

Fig. 5 The present pipe centerline turbulence statistics ($u'_c/\bar{U}_c$, $S_c(u')$, and $F_c(u')$) versus x/D for $3\times10^4 \leq \mathrm{Re}_c \leq 8\times10^4$ ($2.63\times10^4 \leq \mathrm{Re}_m \leq 7\times10^4$) and 0% tripping

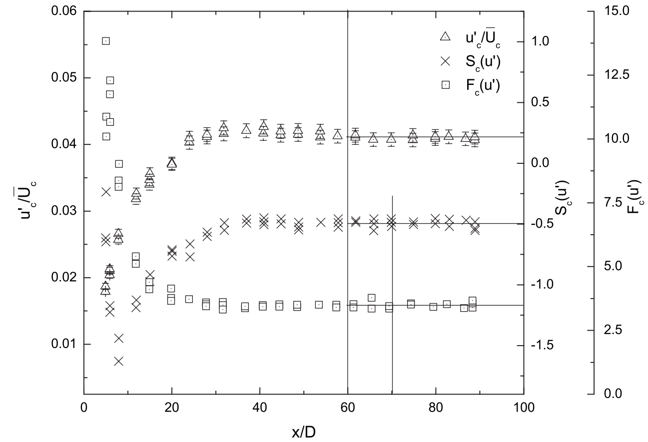

Fig. 6 The channel centerline turbulence statistics ($u'_c/\bar{U}_c$, $S_c(u')$, and $F_c(u')$) versus x/D for $\mathrm{Re}_m=10^4$ and 20% tripping [24]

present paper use rather the centerline statistics as representative of the turbulent motion to show that the flow is Reynolds number independent or does not depend further on the streamwise coordinate, x. The authors believe that reaching the constant behavior of the turbulence statistics at the pipe or at the channel centerline (i.e., the last station of turbulence across the pipe or the channel cross sectional area) is enough to state that flow is fully turbulent and intermittency disappears.

Hence, to provide an answer for the above question, the time-averaged properties of a turbulent flow are to be described by their statistical moments $\overline{M^n}$, and consequently a spatially fully developed turbulent flow is assumed if all statistical moments of the flow show invariant behavior under translation, i.e.,

$$\frac{\partial \overline{M^n}}{\partial x} = 0, \qquad \forall\, x_1 > x_{1,v} \tag{6}$$

where $x_{1,v}$ can be determined experimentally by conducting intensive turbulence measurements through the flow field along the streamwise direction. The above equation represents, therefore, a good criterion to fulfill the assumption of the full development state of the flow either in the pipe or in the channel by carrying out intensive centerline measurements at different x-wise positions. This approach turns out to be in close agreement with the criteria introduced by Patel and Head [21], and recently by Zagarola and Smits [13].

In the current phase of the experimental study, the HWA and the LDA have been utilized for evaluating, quantitatively, the mean flow characteristics and the turbulence statistics in both the pipe and the channel facilities. A precise location of the hot wire at the pipe centerline was of vital importance, and therefore great care was taken to ensure a correct positioning of the wire. Hence, a calibration positioning procedure proposed by Bhatia et al. [32] and Durst et al. [33] was applied to position the wire. Without triggering the flow at the pipe entrance, i.e., turbulence was developed naturally, efforts have been therefore concentrated to provide an answer for the following question: How does the inlet flow conditions and the measuring locations influence the transition from the laminar to turbulent flow regime?

Flow transition to turbulence through the pipe was detected via the centerline measurements in similar way to the channel flow data of Fischer [24]. The available channel flow data [24], with and without triggering the flow at the channel inlet section, were utilized to perform the comparative study versus the present pipe results. A summary of the centerline measurements (i.e., ($u'_c/\bar{U}_c$), $S_c(u')$, and $F_c(u')$) in both the pipe and the channel test sections for different streamwise distances, x/D, is presented in Figs. 5 and 6. Figure 5 indicates that a pipe fully developed turbulent flow could be achieved for a transition length $x/D \geq 60$ and high enough Reynolds number (i.e., $\mathrm{Re}_m \geq 2.63\times10^4$), supporting Patel and Head's [21] conclusion, and turned out to be in good agreement with Zagarola and Smits [13]. Similar channel centerline measurements by 20% tripping have been carried out [24] at different x/D from the channel input, and data are presented in Fig. 6 for $\mathrm{Re}_m=10^4$. Both figures, i.e., Figs. 5 and 6, clearly show independence of the streamwise turbulence characteristics on a streamwise distance of $x/D \geq 60$ either for the circular pipe or the rectangular channel facilities. A constant behavior for both the centerline skewness $S_c(u')$ and flatness $F_c(u')$ factors was also observed; however, for a relatively long entrance length $x/D \geq 70$, i.e., $S_c(u')=-0.51$ and $F_c(u')=3.5$, which are very close to values for isotropic and homogeneous turbulence [34]. As a result, for $x/D \geq 70$, it might be concluded that there is no systematic dependence of the flow properties on the streamwise distance anymore, and therefore the state of full development of the flow was achieved.

Based on a conclusion deduced from Fig. 6, Fischer [24] carried out, for various tripping ratios and Reynolds numbers, all his channel measurements at a fixed station $x/D=80$ from the channel input that assured no dependence on the streamwise distance (x/D). On the other hand, the pipe flow measurements were carried out at different measuring locations and for various input velocities without triggering the flow. Figures 7 and 8 present the mean flow results in both the pipe for $x/D \geq 54.6$ and the channel at $x/D=80$, showing the ratio of the centerline-average-velocity to the bulk flow velocity versus the centerline-average-velocity and the bulk-velocity based Reynolds numbers. Figure 7 clearly shows almost a constant behavior of $\bar{U}_c/\bar{U}_b$ for long enough pipe test section, $x/D \geq 54.6$, and for high enough Reynolds number, $\mathrm{Re}_c \geq 3\times10^4$ ($\mathrm{Re}_m \geq 2.63\times10^4$). A similar behavior can be observed in Fig. 8; however, with slight and monotonic decrease in the ratio $\bar{U}_c/\bar{U}_b$ versus the Reynolds number for $\mathrm{Re}_c \geq 3\times10^3$ ($\mathrm{Re}_m \geq 2.46\times10^3$), reaching an asymptotic behavior for $\mathrm{Re}_c \geq 10^4$ ($\mathrm{Re}_m \geq 8.2\times10^3$).

Figures 9 and 10 present selected samples from the results in both the pipe and the channel flows for $x/D \geq 62.4$ and $x/D=80$, respectively, showing the inner scaling of the mean-velocity profiles for different Reynolds numbers. Figure 9 clearly shows that the mean-velocity distribution over the cross section of the pipe collapsed into a single curve for high enough Reynolds number

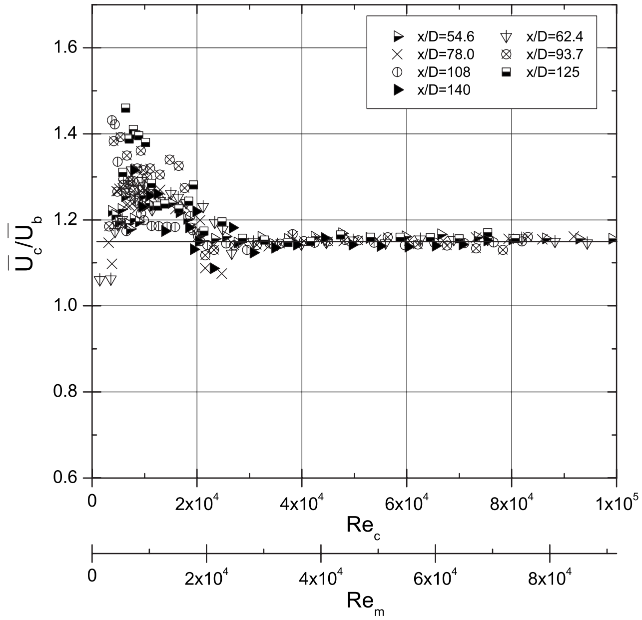

Fig. 7 The ratio of the centerline-average-velocity ($\bar{U}_c$) to the bulk flow velocity ($\bar{U}_b$) versus the centerline-average-velocity and/or the bulk-velocity based Reynolds numbers in the pipe flow for various measuring locations (x/D)

$Re_m \geq 4\times10^4$ ($R^+ \geq 1040$), and long enough entrance length $x/D \geq 62.4$ when the mean-velocity data are scaled with the wall friction flow velocity, u_τ, and the wall distance scaled with the viscous length scale, $l_c=\nu/u_\tau$. Both figures illustrate clearly that there is a too short or even no real log region since the current experiments have simply too low Reynolds numbers to show a real logarithmic character of the so-called overlap region [35]. In spite of that fact, a satisfactory agreement for the normalized mean-velocity distribution with the logarithmic line, $U^+ = 1/\kappa \ln(y^+)+B$, proposed by Perry et al. [36] with $\kappa=0.39$ and $B=4.42$, Nagib et al. [37,38] ($\kappa=0.384$ and $B=4.127$), and Zanoun et al. [23] ($\kappa=0.384$ and $B=4.43$), might be observed in Fig.

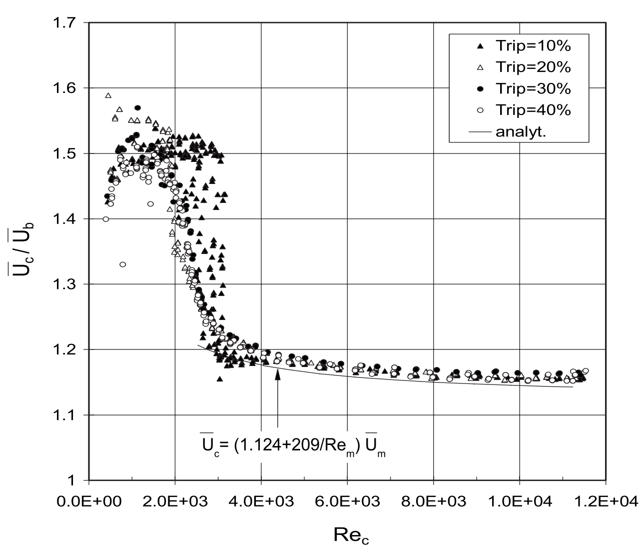

Fig. 8 The ratio of the centerline-average-velocity ($\bar{U}_c$) to the bulk flow velocity ($\bar{U}_b$) versus the centerline-average-velocity based Reynolds number in the channel flow for various tripping ratios [24]

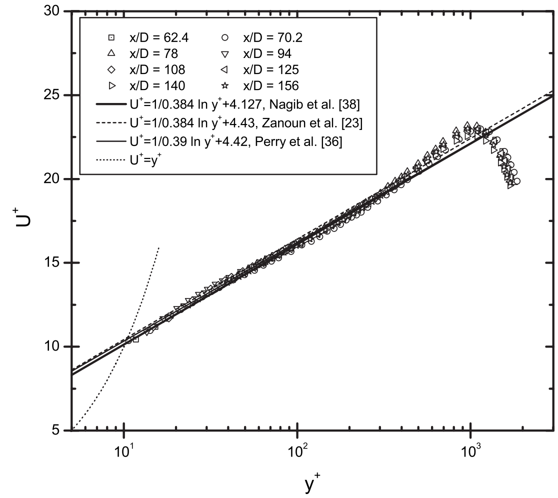

Fig. 9 The inner scaling of the present pipe mean-velocity profiles for $1040 \leq R^+ \leq 1140$

9. The mean-velocity data of Fischer [24] obtained using the LDA were presented in Fig. 10, showing poor agreement with the channel logarithmic line, proposed by Zanoun et al. [31] with $\kappa=0.37$ and $B=3.7$. On the other hand, a satisfactory agreement might be obtained for Fischer's higher Reynolds number data [24] (i.e., $R^+ \approx 481$) with the logarithmic line when higher values for both constants, i.e., $\kappa=0.41$ and $B=5.5$, are used; see also Fig. 4.12 in Ref. [24] for more details. Therefore, it appears from Fig. 10 that Fischer's mean-velocity data [24] did not support the accepted logarithmic velocity profile because of its low range of the Reynolds number. A displacement effect, i.e., velocity overshoot, can be also observed in Figs. 9 and 10 in the region where $y^+ \leq 150$, resulting in deviation from the logarithmic velocity profile that might be interpreted also as a result of the low Reynolds number effect. On the other hand, this bump, i.e., velocity overshoot, in the mean-velocity profile for $10 \leq y^+ \leq 150$ can be interpreted as a local power law similar to the one found by McKeon et al. [35].

Let us now apply the centerline turbulence intensity as a transition indicator or an argument for the state of flow full development. The pipe centerline-velocity fluctuations were measured for various Reynolds numbers, $Re_c \leq 1.2\times10^5$ ($Re_m \leq 106\times10^3$), and entrance lengths, $3.9 \leq x/D \leq 156$, and the results are presented in Fig. 11. It is worth noting again that the present pipe centerline measurements were carried out using the HWA without triggering the flow at the pipe entrance, looking for the transition Reynolds number and flow development as a function of the measuring location and the input flow velocity. The pipe centerline results are then compared with the channel centerline-velocity fluctuations [24] presented in Fig. 12 for $Re_c \leq 1.2\times10^4$ ($Re_m \leq 10^4$). In Figs. 11 and 12, the centerline-velocity fluctuations were scaled with the centerline-average-velocity and presented versus the centerline-average-velocity and/or the bulk-velocity based Reynolds numbers for the pipe and the channel flows, respectively. For the low range of the pipe Reynolds number, i.e., $Re_c \leq 2\times10^4$ ($Re_m \leq 1.76\times10^4$), flow disturbances were not growing fast enough, and therefore flow remained laminar. However, for $Re_c \geq 30\times10^3$ ($Re_m \geq 26.3\times10^3$), flow disturbances grow fast due to the higher growing rate of energy production, resulting in transition to turbulent regime. The channel measurements [24] were carried out at a fixed streamwise distance $x/D=80$, utilizing the LDA, aiming at investigating the effect of tripping the flow on the transition Reynolds number. The tripping device, i.e., an inlet fence, used by Fischer [24] was mounted at the channel entrance, i.e., $x=0$, with height ratios of $2\delta/D$

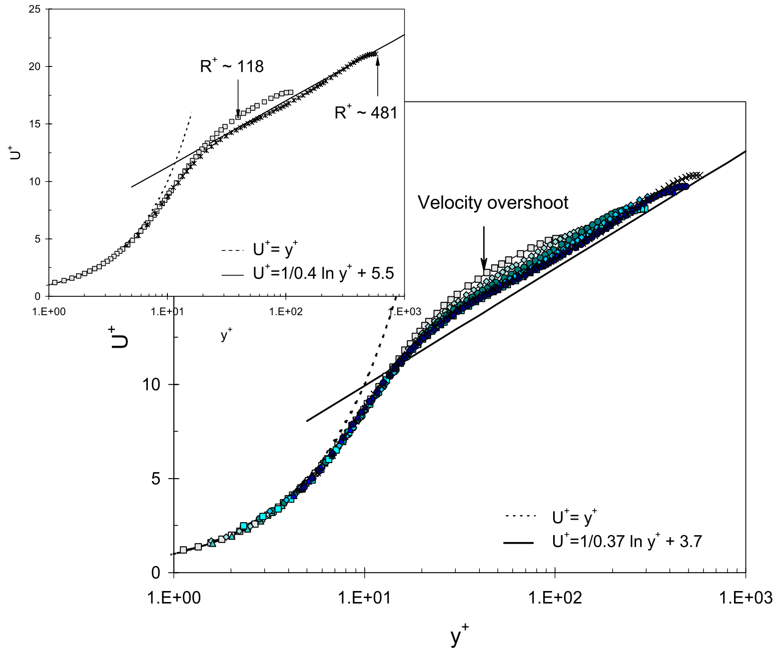

Fig. 10 The inner scaling of the channel mean-velocity profiles for 118 $\leq R^+ \leq 481$ [24]

$=0\%, 10\%, 20\%, 30\%, 40\%$ to trigger the flow over the lower and upper walls of the channel test section. The channel results presented in Fig. 12 were obtained for 0% tripping and for a tripping device with height of $2\delta = (1/10)D$, i.e., 10% of the channel full height. For $\mathrm{Re}_c \leq 2.4\times 10^3$ ($\mathrm{Re}_m \leq 2\times 10^3$), Fischer [2] noticed that the laminar behavior with $2\delta/D \leq 10\%$ tripping stay unaffected, meaning that disturbances were not strong enough to grow in the downstream direction for this range of Reynolds number. On the other hand, for high enough channel Reynolds number, i.e., $\mathrm{Re}_c \geq 10^4$ ($\mathrm{Re}_m \geq 8.2\times 10^3$), the channel flow was fully turbulent either with or without tripping the flow. In spite of the fact that the Reynolds number range in the current pipe and the channel [24] is different, Figs. 11 and 12 show almost the same general characteristics. A similar behavior to the channel flow was observed for the pipe flow, however, along different ranges of the Reynolds number. When the Reynolds numbers are less than the critical values, i.e., $\mathrm{Re}_c \leq 17.5\times 10^3$ ($\mathrm{Re}_m \leq 15.5\times 10^3$) and $\mathrm{Re}_c \leq 2.4\times 10^3$ ($\mathrm{Re}_m \leq 2\times 10^3$) in the pipe and in the channel, respectively, all the initial conditions are attracted to the laminar state, which is the global attractor for both systems. However, if the Reynolds numbers are higher than the above critical values, nearly all the initial conditions give rise to turbulence and the laminar state becomes a local attractor. These arguments are consistent both with Reynolds' original observations [39] and the recent experimental results of Draad et al. [1].

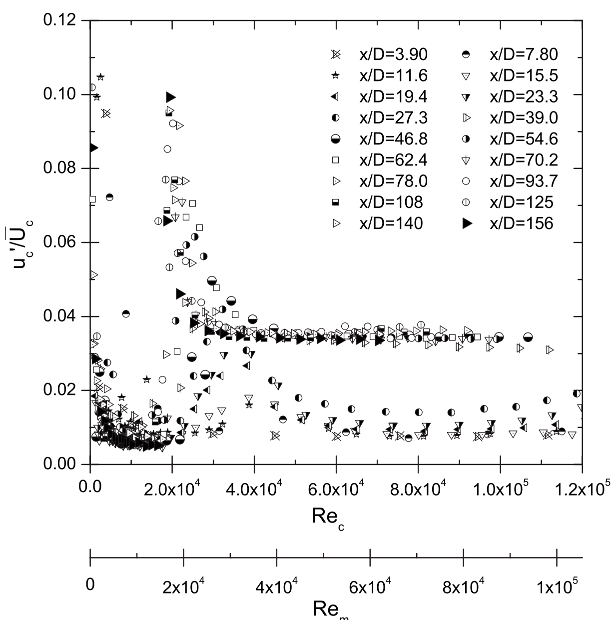

Fig. 11 The present pipe normalized centerline-velocity fluctuations ($u'_c/\bar{U}_c$) for various x/D versus the centerline-average-velocity and/or the bulk-velocity based Reynolds numbers

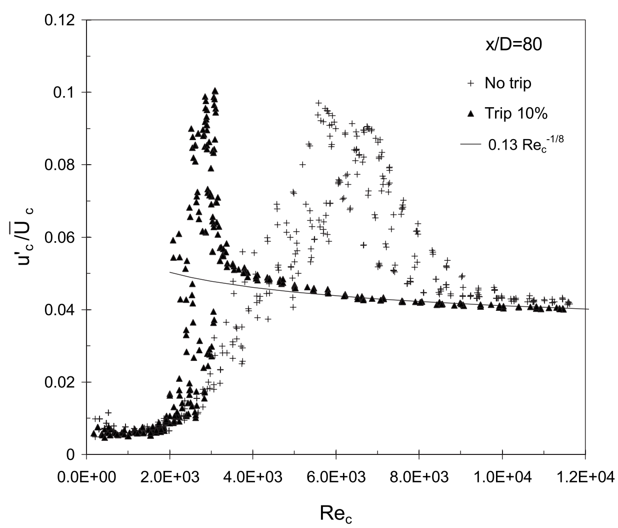

Fig. 12 The channel normalized centerline-velocity fluctuations ($u'_c/\bar{U}_c$) for 0% and 10% tripping versus the centerline-average-velocity based Reynolds number [24]

For the measuring locations at $x/D \leq 27.3$, a wide range of the transition Reynolds number was observed, i.e., $Re_c \approx 17.5 \times 10^3 - 60 \times 10^3$ ($Re_m \approx 15.5 \times 10^3 - 53 \times 10^3$), with lower turbulence intensity level, $u'_c/\bar{U}_c \leq 2\%$. However, for the measuring locations at $x/D \geq 39$, a narrow range of the transition Reynolds number, i.e., $Re_c \approx 17.5 \times 10^3 - 45 \times 10^3$ ($Re_m \approx 15.5 \times 10^3 - 39 \times 10^3$), took place. In other words, for a narrow range of inlet flow velocities, the pipe flow experiments showed that a longer streamwise entrance, i.e., $x/D \geq 39$, is needed to achieve the turbulent flow regime. On the other hand, a shorter pipe entrance, i.e., $x/D \leq 27.3$, might be used, however, with higher input flow velocity or higher Reynolds number, i.e., $Re_c \geq 6 \times 10^4$ ($Re_m \geq 53 \times 10^3$) to reach turbulent flow at earlier measuring position. This came in good agreement with the observation mad by Zagarola and Smits [13], indicating that at high Reynolds numbers the transition length is considerably smaller. After assuring the fully turbulent regime, the turbulent fluctuations, $u'_c/\bar{U}_c$, at the pipe or at the channel centerlines were observed to monotonically decrease, however, slightly with increasing the Reynolds number for $x/D \geq 39$ (see Fig. 11) or for high enough disturbances, i.e., $2\delta/D \geq 10\%$ tripping the flow (see Fig. 12). In case of not tripping the flow at the channel entrance, a wide range of the transition Reynolds number $Re_c \approx 2 \times 10^3 - 2 \times 10^4$ ($Re_c \approx 1.6 \times 10^3 - 8.2 \times 10^3$) existed as can be seen in Fig. 12. On the contrary, all the channel flow measurements collapsed into a single curve and a narrow range of the transition Reynolds number was obtained, $Re_c \approx 2 \times 10^3 - 3.5 \times 10^3$ ($Re_c \approx 1.6 \times 10^3 - 2.8 \times 10^3$), with 10% tripping, and therefore an earlier transition to turbulent flow regime was observed at $Re_c \approx 3.5 \times 10^3$. For the pipe measurements at $x/D = 78$, which is almost equivalent to Fischer's channel measuring location $x/D = 80$ [24], and under the natural transition condition, the pipe transition Reynolds number was found to be $Re_c \approx 28.8 \times 10^3$ ($Re_m \approx 25 \times 10^3$), which is almost three times the transition Reynolds number in the channel flow $Re_c \approx 10^4$ ($Re_m \approx 8.2 \times 10^3$). One can observe also from Figs. 11 and 12 that the maximum turbulence intensity level is around 10% that took place at $Re_c \approx 2 \times 10^4$ ($Re_m \approx 17.5 \times 10^3$) in the pipe, however, for the channel flow under the natural transition occurred at $Re_c \approx 6 \times 10^3$ ($Re_m \approx 4.9 \times 10^3$) and at $Re_c \approx 3 \times 10^3$ ($Re_m \approx 2.4 \times 10^3$) with 10% tripping.

The centerline-velocity fluctuations, $u_c'^2$, are also presented versus the centerline-average-velocity and/or the bulk-velocity based Reynolds numbers in Figs. 13 and 14 for the pipe and the channel flows, respectively. In the pipe flow (Fig. 13), depending on the measuring location (x/D), a transition Reynolds number (Re_c) between 17.5×10^3 and 60×10^3 ($Re_m \approx 15.5 \times 10^3 - 53 \times 10^3$) was observed. An earlier transition for $Re_c \approx 25 \times 10^3$ ($Re_m \approx 22 \times 10^3$) was obtained at larger downstream distance $x/D = 156$, in comparison to $Re_c \approx 45 \times 10^3$ ($Re_m \approx 39 \times 10^3$) for the shorter downstream distance $x/D = 46.8$. One could speculate that at higher input velocities, i.e., at high Reynolds numbers, the flow is more less stable and therefore disturbances are growing fast enough along a short pipe entrance due to the high rate of energy production, resulting in earlier transition to the turbulent regime. At higher Reynolds number, Zagarola and Smits [13] indicated also that the transition length is considerably smaller. On the other hand, for lower values of the inlet flow velocities, a further distant measuring location, i.e., an extended wall distance to amplify disturbances in the downstream direction, leading to transition to the turbulent flow is expected. Nishi et al. [40] obtained a pipe natural laminar-to-turbulent transition at $x/D = 533.3$ for $Re_m = 11.5 \times 10^3$, utilizing Durst and Ünsal's [41] pipe facility, who had a slightly higher value $Re_m = 13 \times 10^3$ for a natural transition. Nishi et al. [40] showed in their paper, Fig. 14, that a strong dependence of the laminar-to-turbulent transition on the measuring position exists, i.e., shorter pipe entrance $x/D = 260$ can achieve the laminar-to-turbulent transition if the time interval between disturbances at the pipe entrance is too small, i.e., applying inlet disturbances with higher frequency. On the other hand, if the time interval is large, a more distant measuring station is needed to achieve the transition to turbulence, similar to the effect of tripping the flow at the channel entrance as can be clearly observed in Fig. 14. For instance, earlier transition to turbulent flow in the channel at $Re_c \approx 2400$ ($Re_m \approx 2000$) took place if the tripping ratio is increased from 10% to 20%.

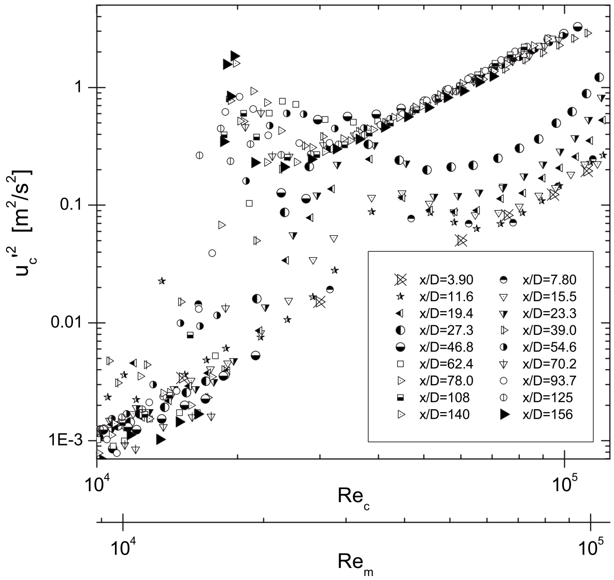

Fig. 13 The present pipe centerline-velocity fluctuations ($u_c'^2$) for various x/D versus the centerline-average-velocity and/or the bulk-velocity based Reynolds numbers

The outcome from Figs. 11–14 in both the pipe and the channel flows could be also obtained by looking at the higher order statistics, i.e., the third and the fourth moments, of the centerline measurements presented in Figs. 15–18. Conclusions extracted from Figs. 15–18 support the transition Reynolds numbers derived from Figs. 11–14 either for the pipe or the channel flows. Figures 15 and 17 clearly show independence of the streamwise turbulence higher order statistics (i.e., the skewness and the flatness), respec-

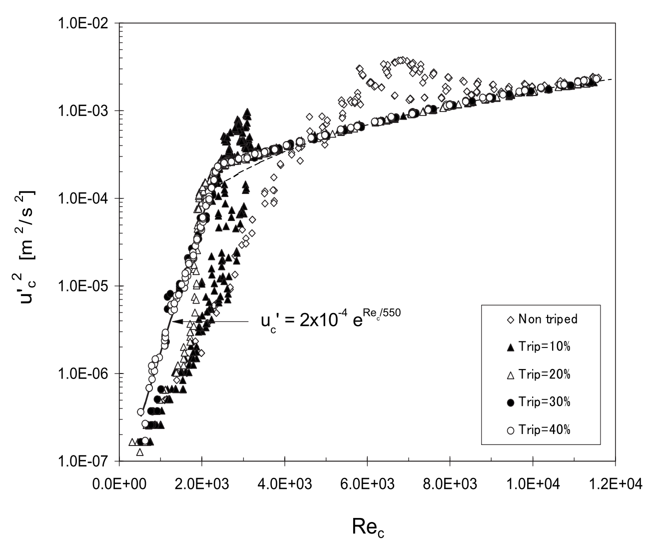

Fig. 14 The channel centerline-velocity fluctuations ($u_c'^2$) for different tripping ratios versus the centerline-average-velocity based Reynolds number [24]

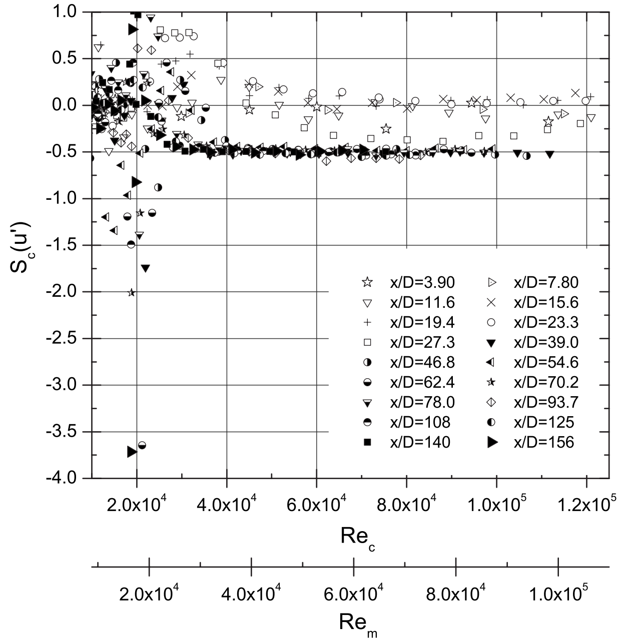

Fig. 15 The present pipe centerline skewness factor for various *x/D* versus the centerline-average-velocity and/or the bulk-velocity based Reynolds numbers

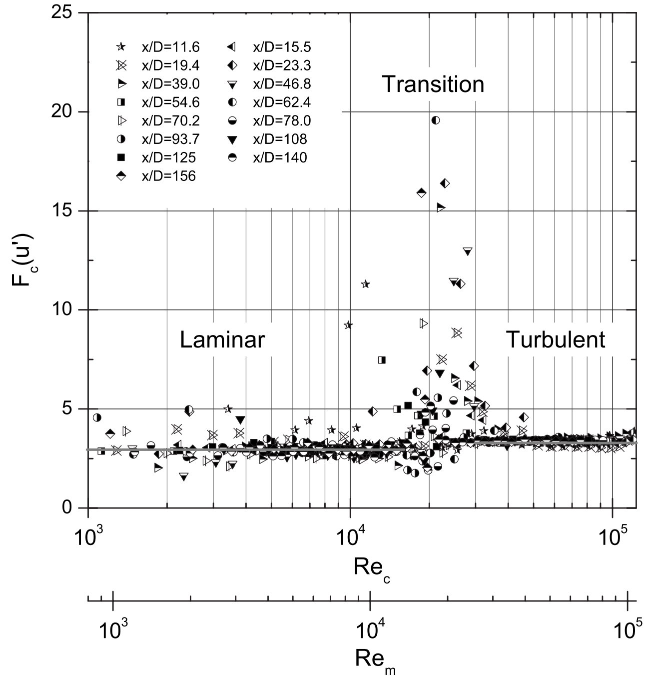

Fig. 17 The present pipe centerline flatness factor for various *x/D* versus the centerline-average-velocity and/or the bulk-velocity based Reynolds numbers

tively, on a streamwise distance of $x/D \geq 39$ for $Re_c \sim 36 \times 10^3$ ($Re_m \sim 3 \times 10^4$) in the circular pipe facility. However, the rectangular channel measurements of Fischer [24] have been carried out at a fixed measuring location $x/D = 80$, selected based on a conclusion derived from Fig. 6. Figures 16 and 18 show also ~~an~~ independent behavior of both the channel streamwise skewness and flatness factors for $Re_c > 3500$ and 10% tripping. A constant behavior for both the centerline skewness $S_c(u')$ (Figs. 15 and 16) and flatness $F_c(u')$ (Figs. 17 and 18) factors was observed, i.e., $S_c(u') \approx -0.51$ and $F_c(u') \approx 3.5$, which are very close to values for isotropic and homogeneous turbulence [34]. As a result, for a pipe streamwise distance $x/D \geq 40$ and high enough Reynolds number $Re_c \geq 45 \times 10^3$ ($Re_m \geq 39 \times 10^3$), it might be concluded that there is no systematic dependence of the pipe flow properties on the x-wise position, and therefore the state of flow full development was achieved.

4 Conclusions

By setting up a small pipe test facility at LAS, BTU Cottbus, we were able to predict the transition Reynolds number for various flow development lengths and inlet flow velocities. A comparative study of the current pipe results versus some available channel data [24] is presented, reflecting effects of flow geometry, entrance flow conditions, and measuring location on the transition Reynolds number. Hence, to well define a criterion for the flow

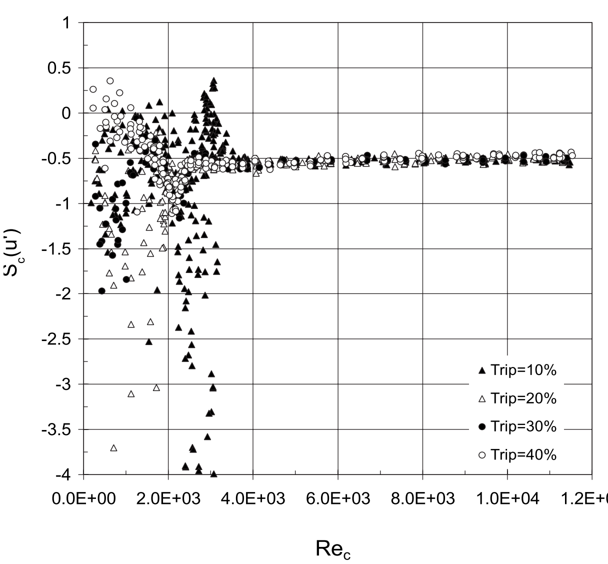

Fig. 16 The channel centerline skewness factor for different tripping ratios versus the centerline-average-velocity based Reynolds number [24]

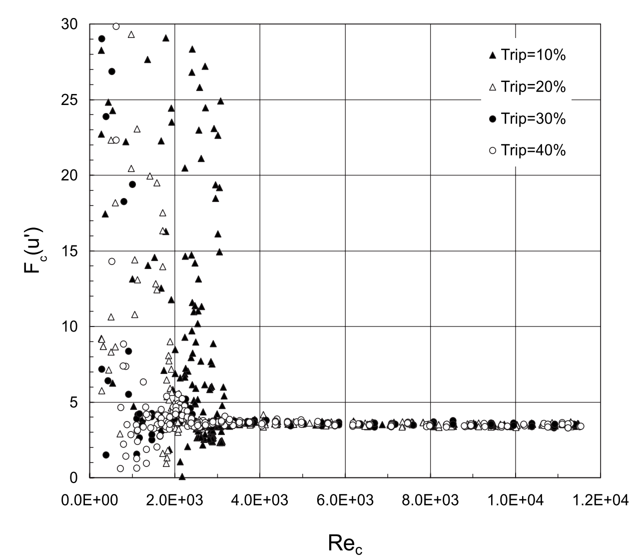

Fig. 18 The channel centerline flatness factor for different tripping ratios versus the centerline-average-velocity based Reynolds number [24]

transition and the state of flow turbulence, the effects of factors such as the entrance length/measuring location (x/D), and the inlet flow conditions, e.g., $\bar{U}_b$ or Re_m, have been taken into consideration, resulting in the following conclusions.

- Without triggering the flow at the pipe entrance, the transition Reynolds number was found to depend on the measuring location, e.g., the natural transition was found to take place for $(\mathrm{Re}_c)_{\mathrm{crit}} \approx 45 \times 10^3$ $[(\mathrm{Re}_m)_{\mathrm{crit}} \approx 39 \times 10^3]$ and $(\mathrm{Re}_c)_{\mathrm{crit}} \approx 25 \times 10^3$ $[(\mathrm{Re}_m)_{\mathrm{crit}} \approx 22 \times 10^3]$ at measuring locations $x/D = 46.8$ and 156, respectively. On the other hand, for the channel flow measurements at $x/D = 80$, the transition Reynolds number was found to depend on the state of flow at the channel inlet test section, e.g., $(\mathrm{Re}_c)_{\mathrm{crit}} \approx 10^4$ $[(\mathrm{Re}_m)_{\mathrm{crit}} \approx 8.2 \times 10^3]$ for the natural laminar-to-turbulent transition, and $(\mathrm{Re}_c)_{\mathrm{crit}} = 2.4 \times 10^3$ $[(\mathrm{Re}_m)_{\mathrm{crit}} \approx 2 \times 10^3]$ for 20% tripping the flow at the channel entrance.
- A laminar behavior was maintained in the present pipe facility up to $\mathrm{Re}_c \approx 17.5 \times 10^3$ ($\mathrm{Re}_m \approx 15.5 \times 10^3$). In addition, a fully developed turbulent pipe flow was achieved at $x/D \geq 60$ for high enough Reynolds number, $\mathrm{Re}_c \geq 45 \times 10^3$ ($\mathrm{Re}_m \approx 39 \times 10^3$), in close agreement with both Patel and Head [21] and Zagarola and Smits [13].
- Based on the channel flow data, it might be concluded that by triggering the flow at the pipe inlet section, the inlet turbulence intensity level will play an important role for flow transition.

In closing, the transition process to turbulence as well as defining a criterion by which the state of the turbulent flow to be specified in the pipe flow are quite complex, and therefore further research on the subject is still needed. For instance, detailed measurements of the velocity and the pressure fields in the entry section of the pipe is needed, taking effects such as alignment of the pipe, smoothness, and geometry of the contraction, as well as the surface roughness of the pipe test section, into consideration. In addition, detailed measurements of the transitional flow using the particle image velocimetry (PIV) are to be performed. This might clarify what causes the reduction in the natural transition Reynolds number with longer entrance pipe test sections.

Acknowledgment

The authors gratefully acknowledge fund received from the Department of Aerodynamics and Fluid Mechanics, BTU Cottbus to carry out the work. Thanks are also due to Professor Franz Durst for his valuable comments on a draft of the manuscript and to Dr.-Ing. Martin Fischer (LSTM-Erlangen) for providing us his channel data. The authors would also like to acknowledge Professor Dr.-Ing. Ennes Sarradj (BTU Cottbus) for allowing us to utilize the aeroacoustic test facility.

References

[1] Draad, A. A., Kuiken, G. D. C., and Nieuwstadt, F. T. M., 1998, "Laminar-Turbulent Transition in Pipe Flow for Newtonian and Non-Newtonian Fluids," J. Fluid Mech., **377**, pp. 267–312.

[2] Monin, A. S., and Yaglom, A. M., 1999, *Statistical Fluid Mechanics: The Mechanics of Turbulence*, Center for Turbulence Research-CTR Monograph Vol. I, English edition, revised, and augmented by A. M. Yaglom, Chap. 4, Stanford University, Stanford/NASA Ames Research Center, Moffett Field, CA.

[3] Faisst, H., and Eckhardt, B., 2003, "Traveling Waves in Pipe Flow," Phys. Rev. Lett., **91**, p. 224502.

[4] Wedin, H., and Kerswell, R. R., 2004, "Exact Coherent Structures in Pipe Flow: Traveling Wave Solutions," J. Fluid Mech., **508**, pp. 333–371.

[5] Hof, B., Juel, A., and Mullin, T., 2003, "Scaling of the Turbulence Transition Threshold in a Pipe," Phys. Rev. Lett., **91**(24), pp. 244502.

[6] Eckhardt, B., Schneider, T. M., Hof, B., and Westerweel, J., 2007, "Turbulence Transition in Pipe Flow," Annu. Rev. Fluid Mech., **39**, pp. 447–468.

[7] Kerswell, R. R., 2005, "Recent Progress in Understanding the Transition to Turbulence in a Pipe," Institute of Physics Publishing, Nonlinearity, **18**, pp. R17–R44.

[8] Willis, A. P., Peixinhoy, J., Kerswell, R. R., and Mullin, T., 2008, "Experimental and Theoretical Progress in Pipe Flow Transition," Philos. Trans. R. Soc. London, Ser. A, **366**(1876), pp. 2671–2684.

[9] Trefethen, L. N., Trefethen, A. E., Reddy, S. C., and Driscoll, T. A., 1993, "Hydrodynamic Stability Without Eigenvalues," Science, **261**, pp. 578–584.

[10] Waleffe, F., 1997, "On the Self-Sustaining Process in Shear Flows," Phys. Fluids, **9**, pp. 883–900.

[11] Wygnanski, I. J., and Champagne, F. H., 1973, "On Transition in a Pipe. Part 1. The Origin of Puffs and Slugs and the Flow in a Turbulent Slug," J. Fluid Mech., **59**, pp. 281–335.

[12] Wygnanski, I. J., Sokolov, M., and Friedman, D., 1975, "On Transition in a Pipe. Part 2. The Equilibrium Puff," J. Fluid Mech., **69**, pp. 283–304.

[13] Zagarola, M. V., and Smits, A. J., 1998, "Mean-Flow Scaling of Turbulent Pipe Flow," J. Fluid Mech., **373**, pp. 33–79.

[14] Nikuradse, J., 1932, "Gesetzmässigkeiten der turbulenten Strömung in glatten Rohren," Forschg. Arb. Ing.-Wes. Heft, **356**, pp. 1–36.

[15] Sarpkaya, T., 1975, "A Note on the Stability of Developing Laminar Flow Subjected to Axisymmetric and Non-Axisymmetric Disturbances," J. Fluid Mech., **68**, pp. 345–351.

[16] Huang, L. M., and Chen, T. S., 1974, "Stability of Developing Pipe Flow Subjected to Non-Axisymmetric Disturbances," J. Fluid Mech., **63**, pp. 183–193.

[17] Huang, L. M., and Chen, T. S., 1974, "Stability of the Developing Laminar Pipe Flow," Phys. Fluids, **17**, pp. 245–247.

[18] Perry, A. E., and Abel, C. J., 1975, "Scaling Laws for Pipe-Flow Turbulence," J. Fluid Mech., **67**, pp. 257–271.

[19] Lien, K., Monty, J. P., Chong, M. S., and Ooi, A., 2004, "The Entrance Length for Fully Developed Turbulent Channel Flow," *15th Australian Fluid Mechanics Conference*, Dec. 13–17, University of Sydney, Sydney, Australia.

[20] Laufer, J., 1953, "The Structure of Turbulence in Fully Developed Pipe Flow," NACA, Report No. 1174.

[21] Patel, V. C., and Head, M. R., 1969, "Some Observations on Skin Friction and Velocity Profiles in Fully Developed Pipe and Channel Flows," J. Fluid Mech., **38**, pp. 181–201.

[22] Doherty, J., Ngan, P., Monty, J., and Chong, M., 2007, "The Developments of Turbulent Pipe Flow," 16th Australian Fluid Mechanics Conference, Crown Plaza, Gold Coast, Australia, Dec. 2–7, pp. 266–270.

[23] Zanoun, E.-S., Durst, F., Bayoumi, O., and Al-Salaymeh, A., 2007, "Wall Skin Friction and Mean Velocity Profiles of Fully Developed Turbulent Pipe Flows," Exp. Therm. Fluid Sci., **32**(1), pp. 249–261.

[24] Fischer, M., 1999, "Turbulente wandgebundene Strömungen bei kleinen Reynoldszahlen," Ph.D., thesis, Universität Erlangen Nürnberg, Germany.

[25] Sarradj, E., Schulze, C., and Zeibig, A., 2005, "Identification of Noise Source Mechanisms Using Orthogonal Beam Forming," Nov., St. Raphael.

[26] Hof, B., 2004, "Transition to Turbulence in Pipe Flow," *Laminar-Turbulent Transition and Finite Amplitude Solutions*, T. Mullin and R. R. Kerswell, eds., Springer, Dordrecht, pp. 221–231.

[27] Grossmann, S., 2000, "The Onset of Shear Flow Turbulence," Rev. Mod. Phys., **72**(2), pp. 603–618.

[28] Schiller, L., 1922, "Die Entwicklung der laminaren Geschwindigkeitsverteilung und ihre Bedeutung für Zähigkeitsmessungen," Z. Angew. Math. Mech., **2**, pp. 96–106.

[29] Pfeninger, W., 1961, "Boundary Layer Suction Experiments With Laminar Flow at High Reynolds Numbers in the Inlet Length of a Tube by Various Suction Methods," *Boundary Layer and Flow Control*, G. V. Lachman, ed., Pergamon, Oxford, pp. 961–980.

[30] Blasius, H., 1913, "Das Ähnlichkeitsgesetz bei Reibungsvorgängen in Flüssikeiten," Forsch. Arb. Ing.-Wes, , pp. 131–137.

[31] Zanoun, E.-S., Durst, F., and Nagib, H., 2003, "Evaluating the Law of the Wall in Two-Dimensional Fully Developed Turbulent Channel Flows," Phys. Fluids, **15**(10), pp. 3079–3089.

[32] Bhatia, J. C., Durst, F., and Jovanovic, J., 1982, "Corrections of Hot-Wire Measurements Near Walls," J. Fluid Mech., **122**, pp. 411–431.

[33] Durst, F., Zanoun, E.-S., and Pashtrapanska, M., 2001, "In Situ Calibration of Hot Wires Close to Highly Heat-Conducting Walls," Exp. Fluids, **31**, pp. 103–110.

[34] Hinze, J. O., 1975, *Turbulence*, 2nd ed., McGraw-Hill, New York.

[35] McKeon, B. J., Swanson, C. J., Zagarola, M. V., Donnelly, R. J., and Smits, A. J., 2004, "Friction Factors for Smooth Pipe Flow," J. Fluid Mech., **511**, pp. 41–44.

[36] Perry, A. E., Hafez, S., and Chong, M. S., 2001, "A Possible Reinterpretation of the Princeton Superpipe Data," J. Fluid Mech., **49**, pp. 395–401.

[37] Nagib, H. M., Chauhan, K. A., and Monkewitz, P. A., 2007, "Approach to an Asymptotic State for ZPG Turbulent Boundary Layers," Philos. Trans. R. Soc. London, Ser. A, **95**, pp. 755–770.

[38] Nagib, H. M., and Kapil, A. C., 2008, "Variations of von Kàrmàn Coefficient in Canonical Flows," Phys. Fluids, **20**, ~~p.~~ 101518. AQ: #1

[39] Reynolds, O., 1883, "On the Dynamical Theory of Incompressible Viscous Fluids and Determination of the Criterion," Philos. Trans. R. Soc. London, **186**, pp. 123–164.

[40] Nishi, M., Ünsal, B., and Durst, F., 2008, "Laminar-to-Turbulent Transition of Pipe Flows Through Slugs and Puffs," J. Fluid Mech., **614**, pp. 425–446.

[41] Durst, F., and Ünsal, B., 2006, "Forced Laminar to Turbulent Transition of Pipe Flows," J. Fluid Mech., **560**, pp. 449–464.

AUTHOR QUERIES — 007905JFG

#1 Author: Please check page number in Ref. 38.